

## Research Article

# Effect of a Non-Newtonian Load on Signature $S_2$ for Quartz Crystal Microbalance Measurements

Jae-Hyeok Choi,<sup>1,2</sup> Kay K. Kanazawa,<sup>3</sup> and Nam-Joon Cho<sup>1,2,4</sup>

<sup>1</sup> School of Materials Science and Engineering, Nanyang Technological University, 50 Nanyang Avenue, Singapore 639798

<sup>2</sup> Centre for Biomimetic Sensor Science, Nanyang Technological University, 50 Nanyang Drive, Singapore 637553

<sup>3</sup> Department of Chemical Engineering, Stanford University, Stanford, CA 94305, USA

<sup>4</sup> School of Chemical and Biomedical Engineering, Nanyang Technological University, 62 Nanyang Drive, Singapore 637459

Correspondence should be addressed to Nam-Joon Cho; njcho@ntu.edu.sg

Received 12 July 2014; Accepted 27 October 2014; Published 13 November 2014

Academic Editor: Ignacio R. Matias

Copyright © 2014 Jae-Hyeok Choi et al. This is an open access article distributed under the Creative Commons Attribution License, which permits unrestricted use, distribution, and reproduction in any medium, provided the original work is properly cited.

The quartz crystal microbalance (QCM) is increasingly used for monitoring the interfacial interaction between surfaces and macromolecules such as biomaterials, polymers, and metals. Recent QCM applications deal with several types of liquids with various viscous macromolecule compounds, which behave differently from Newtonian liquids. To properly monitor such interactions, it is crucial to understand the influence of the non-Newtonian fluid on the QCM measurement response. As a quantitative indicator of non-Newtonian behavior, we used the quartz resonator signature,  $S_2$ , of the QCM measurement response, which has a consistent value for Newtonian fluids. We then modified De Kee's non-Newtonian three-parameter model to apply it to our prediction of  $S_2$  values for non-Newtonian liquids. As a model, we chose polyethylene glycol (PEG400) with the titration of its volume concentration in deionized water. As the volume concentration of PEG400 increased, the  $S_2$  value decreased, confirming that the modified De Kee's three-parameter model can predict the change in  $S_2$  value. Collectively, the findings presented herein enable the application of the quartz resonator signature,  $S_2$ , to verify QCM measurement analysis in relation to a wide range of experimental subjects that may exhibit non-Newtonian behavior, including polymers and biomaterials.

## 1. Introduction

The quartz crystal microbalance (QCM) has been widely employed as a label-free acoustic sensor to monitor mass changes due to adsorption on a surface [1–4]. QCM applications have been extended to measure viscoelastic macromolecular interactions with the surfaces of fluids including natural and synthetic macromolecules such as DNA [5, 6], proteins [7, 8], microorganisms [9], endothelial cells [10], polymers [11–13], and polyelectrolyte multilayers [14]. Through these studies, QCM measurements have shown that viscoelastic fluids containing macromolecules exhibit different behavior from that of Newtonian fluids.

An early description of the viscoelastically coupled QCM resonator gave an example of measured changes in the frequency and resistance of the liquid-loaded QCM [2, 15]. The Sandia group provided a complete description of the QCM's theoretical and experimental responses [16, 17], with

results for water-glycerol mixtures [16] and water and water-glycerol mixtures [17]. The Kasemo group presented the effects resulting from the electrical conductivity of the liquid [18]. They demonstrated block diagrams of the instrument for studying both the parallel and the series resonance. Increasingly complex mechanical properties of both glassy and rubbery materials have also been studied using impedance analysis [19].

In addition, other groups have reported numerous QCM studies that aim to understand the viscoelastic behavior of macromolecules as a thin film physically adsorbed or chemically conjugated on the QCM substrate [5–8, 11–13, 19–29], or as a viscous liquid remaining on the substrate [30–34]. Recent studies have shown the potential to decouple the mass adsorption-forming thin layer from the fluid viscosity and density [23, 35].

To verify the QCM measurement response for increasingly diverse applications, there has been interest in

the development of methods for initial checks of the instrument. Recently, we developed simple calculations involving the changes in the resonator properties when loaded by a liquid, which yield fixed values when the resonator is loaded with a Newtonian liquid. We refer to these simple calculations as signatures,  $S_1$  and  $S_2$ . For a given resonator, these signatures were found to have fixed values, independent of the fluid density and viscosity [36].  $S_1$  was calculated from the changes in resonant frequency and resistance at the resonance of the quartz microbalance as follows:

$$S_1 = \frac{|\Delta f|}{\Delta R}, \quad (1)$$

where the magnitudes of  $\Delta f$  and  $\Delta R$  are the changes in the resonant frequency and resistance, respectively, when loaded with the fluid.  $S_1$  can be expressed simply in terms of some fixed properties of the quartz resonator, such as the shear modulus, the electrical capacitance, and the fixed geometrical values of the thickness and electrode area [36]. As an example, the value for one type of simple 5 MHz resonator yielded a value of  $S_1 = 2.03$  under a Newtonian liquid load. This required measurement methods to obtain the values of the resonant frequency and resistance of the resonator, such as impedance analysis [37, 38] or amplitude sensitive oscillators.  $S_2$  was a signature calculated from the changes in the resonant frequency and energy dissipation (or change in  $Q$ ) of the resonator when loaded with a Newtonian fluid:

$$S_2 = \frac{|\Delta f|}{N\Delta D} = \frac{f_{1U}}{2}, \quad (2)$$

where the magnitudes of  $\Delta f$  and  $\Delta D$  are the changes in the resonant frequency and energy dissipation, respectively, and  $N$  is the harmonic number. In the case of  $S_2$ , the value for such a loading turns out to be simply one-half of the unloaded fundamental resonator frequency. For the quartz resonator,  $N$  can take on odd values. The use of measurement devices such as the commercial Q-Sense device made these determinations very convenient and it was possible to identify the change at several harmonic frequencies. Hence, due to the convenience of measuring  $S_2$ , we concentrate on studies related to  $S_2$  in this study. Using the same simple 5 MHz type resonators used for the  $S_1$  tests, the value of  $S_2$  was then 2.5 MHz [36].

$S_1$  and  $S_2$ , calculated from the measured values, served as effective indicators of the proper instrument behavior when the resonator was loaded with a Newtonian fluid. The values of  $S_1$  and  $S_2$  were found to be very close to the measured values when using a Newtonian fluid such as ethanol or water. However, when a liquid-polymer mixture fluid was used, deviations from those values appeared. The deviations from the constant value became larger as the mass fraction of the polymer mixture increased. These deviations might arise from the non-Newtonian character of the mixtures at large volume concentrations of polymer.

To evaluate and analyze the value of  $S_2$  in QCM measurements involving macromolecules, we used polyethylene glycol (PEG) as a model system because the molecular

weight can be varied and it has high solubility [37–39]. For PEG monomers in the molecular weight range between 200 and 20000 Da, PEG monomers with an average molecular weight of 400 Da (PEG400) were selected for our experiments because it shows both Newtonian behavior at lower concentrations and non-Newtonian behavior at higher concentrations [13, 24, 28]. Once the experimental  $S_2$  values were collected, we investigated whether the  $S_2$  values from the theoretical viscoelastic non-Newtonian model, modified from De Kee's three-parameter model [40], could be fit to the experimental values of  $S_2$  to verify whether the application of  $S_2$  can be extended to the initial system check-up indicator for non-Newtonian fluids.

## 2. Materials and Methods

**2.1. Materials.** Polyethylene glycol (PEG) was purchased from Sigma-Aldrich Co. LLC. (product number 202398). As the average molecular weight ( $M_n$ ) of the PEG is 400 Da, it is referred to as PEG400 in this study. The density of PEG400 is 1.128 g/mL and its melting point is 4–8°C. PEG400 was diluted with 10 mM Tris buffer with 100 mM NaCl, pH 7.4, in MilliQ-deionized water with high resistivity (MilliPore, Oregon, USA). The PEG400 was diluted according to the volume concentration (%) from 1% to 100%. To homogenize PEG400 with buffer, the mixture was vortexed for several minutes. Immediately before experiment, the solution was vortexed again to ensure the PEG400 solution was fully homogenized. All bubbles were excluded before solution injection for measurements.

**2.2. QCM Substrate.** Silicon oxide-coated quartz crystal substrates (QSX303) for QCM measurements were obtained from Q-Sense (Göthenburg, Sweden). The cleaning procedure for the silicon oxide substrates was as follows. First, the silicon oxide substrates were cleaned with 1% SDS and rinsed with ethanol. Second, they were rinsed with deionized water and then with ethanol. Next, they were dried with nitrogen air. Finally, the substrates were exposed to oxygen plasma treatment at maximum power (Harrick Plasma, Ithaca, NY, USA) for 1 minute immediately before experiment.

**2.3. Quartz Crystal Microbalance (QCM).** The Q-Sense E4 instrument from Q-Sense (Göthenburg, Sweden) was used for measurements. This instrument measures the change in the resonance frequency,  $\Delta f$ , and the energy dissipation,  $\Delta D$ , when the volume concentration (%) of PEG400 in 10 mM Tris buffer with 100 mM NaCl, pH 7.4, in MilliQ water increased from 1% to 70%. From 1% to 10%, the volume concentration (%) of PEG400 increased by 1% every 15 minutes. From 10% to 70%, it increased by 10% in every 20–25 minutes [41]. At the fundamental frequency, 5 MHz, an AT-cut piezoelectric crystal was excited at the 3rd, 5th, 7th, 9th, and 11th overtones (15, 25, 35, 45, and 55 MHz in order) and  $\Delta f$  and  $\Delta D$  were measured. After the initial measurement in air, 10 mM Tris buffer with 100 mM NaCl and pH 7.4 was injected for the initial stabilization of the QCM signals. As the volume concentration (%) of PEG400 increased the  $f$  and  $D$  in

the higher overtones became unstable. Therefore, only the stable data are shown in the QCM results. However,  $f$  and  $D$  at the 3rd, 5th, and 7th overtones were stable until the end of the experiment with 70% PEG400.

**2.4. Rheometry.** A Physica MCR 501 stress-controlled rheometer (Anton Paar GmbH, Graz, Austria) was used at a fixed temperature of 24°C in order to measure the viscosity of PEG400 solutions in the volume concentration range of 1% to 100% as a unit of cP. At the same volume concentration (%) of PEG400 solutions, the viscosities were measured at the shear rate, 1 S<sup>-1</sup>. The viscosities were measured at least three times for each volume concentration of PEG400.

### 3. Results and Discussion

**3.1. Modification of Viscoelastic Non-Newtonian Model.** A useful description for a Maxwellian fluid was provided in [42]. Here, we modify the corresponding analytical description by taking into account the De Kee expression. A Maxwellian fluid exhibits Newtonian behavior at very low frequencies but exhibits energy storage, or elastic, behavior at high frequencies and can therefore be represented as follows:

$$\tilde{\eta}_L = \frac{\eta_{DC}}{(1 + j\omega\tau)^\beta}. \quad (3)$$

$\tilde{\eta}_L$  is a complex quantity that represents the complex viscosity of the Maxwellian fluid, and  $\tau$  is the relaxation time for the liquid-elastic mixture. At frequencies where  $\omega\tau$  is negligibly small, the complex viscosity reduces to the constant value of  $\eta_{DC}$ , which is the DC value of the fluid viscosity. In this low frequency regime, the behavior reduces to that for a Newtonian liquid. The quantity  $\beta$  is a parameter that allows for a distribution of relaxation times. When  $\beta = 1$ , the expression for  $\tilde{\eta}_L$  reduces to that of a simple Maxwellian liquid with a single relaxation time. This analytical description of a Maxwellian fluid suggested that we could analyze the behavior of a Maxwellian fluid in the quartz resonator. Based on the De Kee expression, (3) includes the parameter  $\beta$ , which is more complex than the expression for a Maxwellian liquid, given, for example, by equation (14) in [40]. We now consider the effects of these parameters on the rheological properties of the liquid:

$$G_f = \frac{i\omega\eta_f}{1 + i\omega\tau}. \quad (4)$$

Here,  $G_f$  is the complex shear modulus,  $\omega$  is the angular frequency,  $\eta_f$  is the low frequency constant viscosity, and  $t$  is the relaxation time. Comparing it to (3), it can be seen that (4) is represented in terms of the shear modulus rather than the viscosity but otherwise shows the same dependence on the low frequency viscosity and the relaxation time. There is also the absence of a  $\beta$  term, which indicates that a simple Maxwellian fluid is characterized by a single relaxation time  $\tau$ . This is shown here only to demonstrate that the De Kee expression reduces to that for the simple Maxwellian liquid when  $\beta = 1$ .

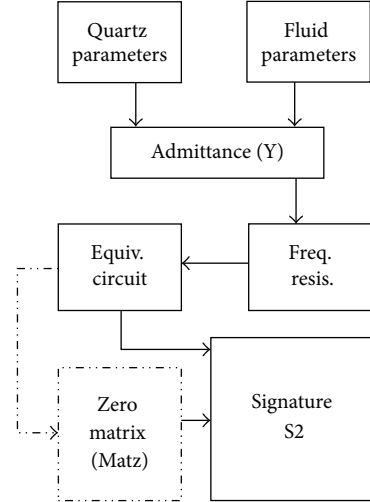


FIGURE 1: Block representation of the various subroutines used in the detailed calculations.

It is not our intention to show that when fluid mixtures are used, the deviations from  $S_2$  result from the fact that the fluid is Maxwellian. It is very unlikely that a given non-Newtonian fluid is purely Maxwellian. Nor do we intend to provide a detailed description of the non-Newtonian nature of the fluid mixture. The purpose of this study is to demonstrate that the experimental variations in  $S_2$  exhibit the types of behavior that would be consistent with the fluid exhibiting both liquid and elastic properties, similar to that which a simple Maxwellian fluid might exhibit, and that  $S_2$  can more broadly serve as an effective measure of the proper operation of the experimental instrument.

**3.2. Block Diagram of Calculations.** Rather than attempting to find an analytical solution for the  $S_2$  signature with the use of a Maxwellian liquid, we decided to use a computational approach. For all viscoelastic materials, there exists a decay length for the shear wave. A fundamental assumption in the computational approach is that the thickness of the liquid applied to the QCM is much greater than this frequency-dependent decay length of the shear wave in the liquid. We assume that the decay length in the fluid is small enough that the approximation of infinite thickness can be taken for the liquid. A diagram of the basis of the theoretical calculations is shown in Figure 1.

The various parameters describing the quartz and the liquid are first input into the program. The first subroutine is for calculating the electrical admittance of the QCM resonator at any arbitrary frequency. A modified Butterworth van Dyke equivalent circuit is used to model the crystal [43]. A simplified representation of this circuit is shown in Figure 2. The equivalent circuit consists of the elements representing the unloaded quartz resonator and the elements representing the viscoelastic fluid. The unloaded resonator consists of three elements,  $L$ ,  $C_s$ , and  $R$ .  $L$  and  $C_s$  yield the resonant frequency of the unloaded QCM through the relation  $\omega_U LC_s = 1$ .  $R$  represents the losses inherent in

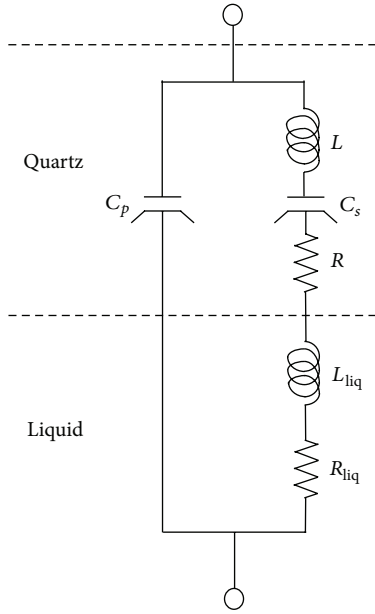


FIGURE 2: Simplified Butterworth van Dyke equivalent circuit used to represent the QCM circuit loaded with a viscoelastic liquid.

the resonator, even when unloaded. The energy dissipation of the unloaded resonator can be expressed in terms of  $R$  through the relation,  $D = R/(\omega_U L)$ .

The first calculation is to determine the values of the resonant frequency, the resistance, and the dissipation for the unloaded resonator. This step is necessary because the calculations involve the changes in the measured values of the resonant frequency and dissipation, with the changes defined as the difference between the measured values when under load and unloaded, respectively. The unloaded values are obtained by setting the appropriate value of the quartz thickness  $dQ$  and the effective electrical contact area in the values for the quartz parameters and to set as a value of zero density for the liquid film parameters. The admittance is calculated, and the resonant frequencies and resistance at the various harmonics are calculated in the “Freq Resis” block. The equivalent circuit parameters are then calculated to yield the values of the resonant frequency, resistance, and dissipation of the zero matrix, Matz. Zero matrix is shown in dash-dot outline in Figure 1 to indicate that it is the initial calculation. As stated earlier, the value of  $S_2$  for loading under a Newtonian fluid was found to be half of the unloaded resonant frequency. As the values of the physical parameters of the quartz resonator are fixed, only the thickness can be varied to change the resonant frequency of the QCM. The thickness of the quartz resonator was chosen so that at the low frequency limit of  $S_2$  (the Newtonian limit), the value of  $S_2$  was in basic agreement with the measured value.

To calculate the resonant frequencies, resistance, and dissipation when the QCM is loaded with a fluid, the parameters of the fluid are entered in the block “Fluid Params.” These parameters include the density and complex viscosity of the fluid mixture. Once the relevant resonant frequencies and resistance and/or dissipation are obtained, the calculations

TABLE 1:  $S_2$  values calculated from the experiment for polyethylene glycol (PEG400) with the titration from 0% to 70% volume concentration.

Volume % (PEG400)	3rd overtone	5th overtone	7th overtone	9th overtone
0%	2.397	2.351	2.394	2.415
5%	2.420	2.415	2.380	2.450
10%	2.445	2.389	2.436	2.453
20%	2.443	2.390	2.396	2.421
30%	2.419	2.378	2.365	2.383
40%	2.402	2.320	2.327	2.303
50%	2.382	2.291	2.267	2.236
60%	2.352	2.195	2.200	2.138
70%	2.296	2.184	2.137	2.011

for the signature can proceed. Instead of characterizing the relaxation time by the variable  $\tau$ , a characteristic transition angular frequency  $\omega_T$  is defined by  $\omega_T \tau = 1$ . By changing the frequency from the angular frequency  $\omega$  to the true frequency,  $f$ , (3) can be written as

$$\tilde{\eta}_L = \frac{\eta_{DC}}{(1 + j(f/f_T))^\beta}. \quad (5)$$

The variable  $f_T$  in (5) is a transitional frequency characterizing the non-Newtonian nature of the fluid. It is convenient to use this variable as a parameter because it relates directly to the test frequency,  $f$ .

**3.3. QCM Measurements.** The QCM measurements were first recorded in air and then in Tris buffer solution only, as shown in Figures 3(a) and 3(b). The QCM measurements continuously monitored the changes in frequency and energy dissipation. Figure 3 shows the rapidly increasing changes in frequency and energy dissipation when higher volume concentrations (%) of PEG400 were injected. After rapidly increasing, both the frequency and dissipation signals stabilize and become constant. The volume concentration of PEG400 increased by 1% every 15 minutes from 0% up to 10%. From 10% to 70%, the concentration increased by 10% every 20–25 minutes. Once the concentration of PEG400 reached 10%, more time was allowed to stabilize the changes in frequency and dissipation. The change in frequency negatively increased but that of energy dissipation positively increased. The trends were similar but in the opposite direction. Based on the shifts in frequency and energy dissipation corresponding volume concentration of PEG400 in the solution, the  $S_2$  value at each overtone number was determined in accordance with (2).

It was clearly observed that the values of  $S_2$  changed according to the changes in the volume concentration and resonant frequency as follows. The first observation is that the value of  $S_2$  decreased at the same resonant frequency as the volume concentration of PEG400 increased, as shown in Table 1. The second observation is that as the volume concentration of PEG400 increased, the value of  $S_2$  decreased as the resonant frequency (or the order of overtones) increased,



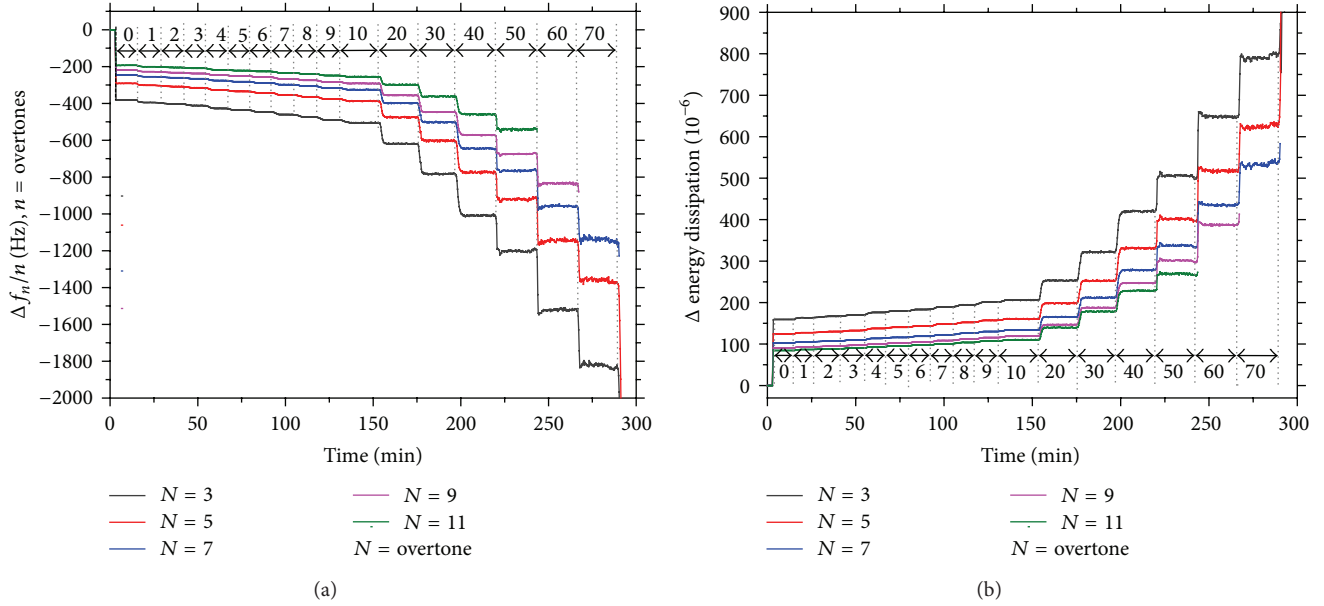


FIGURE 3: Changes in (a) frequency and (b) energy dissipation over time obtained from the QCM-D experiment. PEG400 was injected in increments from 1% to 70% volume concentration. The injected volume concentration of PEG400 in each time period is marked on the graph.

at the same volume concentration of PEG400, as shown in Table 1. The trend of the first observation for  $S_2$  is similar to that reported by Wang et al. [28] using solutions of PEG with the same molecular weight, but they did not specify which resonant frequency or overtone their observation applied to, and only one value per concentration of PEG400 was shown. Therefore, our second observation is a unique result. The values of  $S_2$  at overtone  $n = 3$  (15 MHz) for 50%~70% PEG400 are offset from the main trend in the values of  $S_2$  at the same concentration, for the full range of concentrations. The same trends are also observed at other overtones.

**3.4. Application of the Modified Non-Newtonian Model.** We next compared the experimentally obtained  $S_2$  values with theoretically calculated  $S_2$  values that were computed based on the block diagram in Figure 1 (see [43] for specifics of the algorithm). De Kee's model has three parameters,  $f_T$ ,  $\beta$ , and  $\eta_{DC}$ , and was taken into account in the calculations. Specifically, the simplest De Kee's model was used where  $\beta = 1$  (the Maxwellian fluid model). It describes a fluid with a single transition frequency, as described above in the theoretical results. The fluid data used for the modeling is shown in Table 2. The first and second columns present the volume concentration and density of PEG400-water mixtures, respectively. The density values (in  $\text{kg}\cdot\text{m}^{-3}$ ) were interpolated from data taken from general references. The third column is the viscosity of the fluid mixture in Pa-s measured by rheometry. The final column presents the only variable,  $f_T$ , that was chosen freely as an input in order to obtain a good fit with the experimental data.

In this last column, the 0% value had a very high value of  $f_T$  in order to emulate a Newtonian fluid over the range of frequencies. The values for 5% and 10% were also very high and resulted in the fluids still having a frequency

TABLE 2: Variables used for the theoretical calculations.

Volume % (PEG400)	Density ( $\text{kg}\cdot\text{m}^{-3}$ )	DC viscosity, $\eta_{DC}$ (Pa-s)	Transition frequency, $f_T$ (MHz)
0%	999.70	0.000640	1E12
5%	1086.53	0.000727	5E10
10%	1108.87	0.000995	5E10
20%	1117.51	0.001315	6000
30%	1120.29	0.002032	3000
40%	1121.09	0.003137	800
50%	1121.45	0.004813	500
60%	1121.60	0.007697	330
70%	1121.70	0.011300	250

independent of  $S_2$ , similar to that of a Newtonian liquid. The remaining values of  $f_T$  were taken to yield theoretical values that approximate the measured values of  $S_2$ . The variations of density and DC viscosity are shown in Figure 4. While the change in the density is only small to moderate, the DC viscosity is seen to change strongly with the fluid volume concentration. In any case, these variations were taken into account in the theoretical modeling for  $S_2$ . The experimental results are compared to the theoretical calculations for  $S_2$  in Figure 5.

The experimental values for  $S_2$  are not constant but change with the resonant frequency as described above for mixed fluids. The theoretical plots show the variation of  $S_2$  with resonant frequency for a fluid that has the characteristics described by the simple De Kee relation. While the symbols do not lie directly on the theoretical curves, it is clear that if a simple model with a single transition frequency is used for each fluid mixture, the major

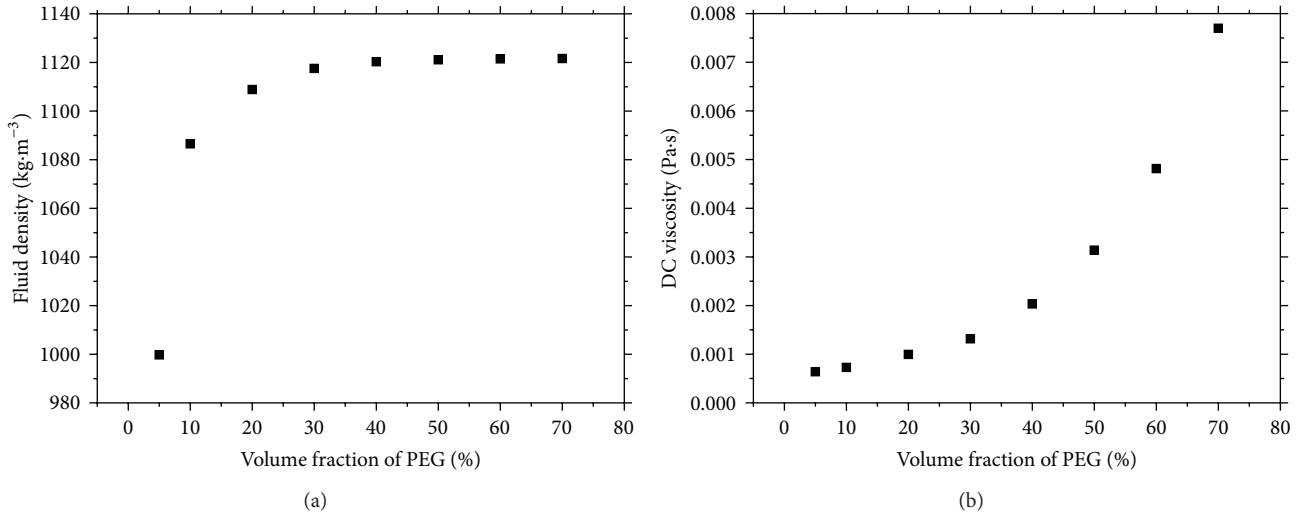


FIGURE 4: Variations in (a) fluid density and (b) DC viscosity as a function of the PEG400 volume concentration.

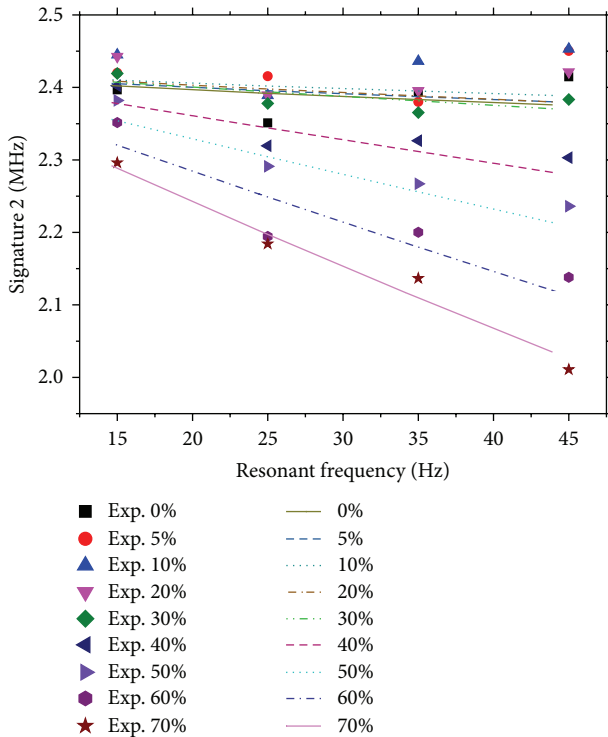


FIGURE 5: Comparison between theoretical calculations and experimental values of  $S_2$ . The lines show the theoretical calculations of  $S_2$ , while the symbols represent the experimental values of  $S_2$ .

behavior of the experimental points is reproduced, including the decrease in the values of  $S_2$  with increasing frequency and the values at the lowest resonant frequency studied (the third harmonic). These decreases take place both as a function of the resonant frequency and as a function of the increasing volume concentration of PEG400. We believe that such behavior indicates the correctness of the assumption not only that the non-Newtonian nature of the fluid is the

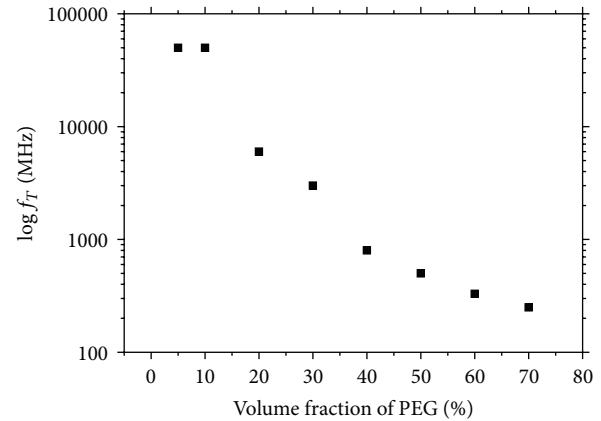


FIGURE 6: Values of  $f_T$  used in the theoretical calculations for each PEG400 volume concentration. The values taken for  $f_T$  vary rather smoothly over the range of concentrations.

origin of the variation in  $S_2$ , but also that the instrument used for the QCM measurements was operating properly. At the higher concentrations of PEG400, the fluid had a decreasing transition frequency, as presented in Figure 6. Modeled as a Maxwellian (single transition frequency) fluid, the mixture becomes more viscous as the concentration of PEG400 increases as anticipated.

#### 4. Conclusions

The calculations obtained from a model that included the mixture of a complex Maxwellian fluid with the solvent agreed reasonably well with several types of behavior of the observed variations in  $S_2$ . Specifically, the low frequency and mass density mixture showed a limiting value toward the constant, representing a Newtonian fluid at the lowest frequencies. With increasing frequency, the decrease in the value of  $S_2$  was reasonably represented by the calculations,

although it should be emphasized that it is the general behavior that is reproduced, not the detailed behavior. The calculated values of  $S_2$  decreased both with increases in the resonant frequency and with increases in the content of the Maxwellian fluid or viscosity. The amount of the experimental changes was in reasonable agreement with the calculated values. We believe that this study provides fairly strong evidence that one major source of the deviations of  $S_2$  from the constant value expected for Newtonian fluids is the addition of an elastic component to the fluid viscoelasticity. In addition, if PEG400 is used as a measurement standard, the measured values of  $S_2$  can be used as a check on the proper operation of the instrument over the frequency range used.

## Conflict of Interests

The authors declare that there is no conflict of interests regarding the publication of this paper.

## Acknowledgments

The authors acknowledge support from the National Research Foundation (NRF-NRFF2011-01), the National Medical Research Council (NMRC/CBRG/0005/2012), and Nanyang Technological University to Nam-Joon Cho.

## References

- [1] M. Cassiède, J.-L. Daridon, J. H. Paillol, and J. Pauly, "Characterization of the behaviour of a quartz crystal resonator fully immersed in a Newtonian liquid by impedance analysis," *Sensors and Actuators A: Physical*, vol. 167, no. 2, pp. 317–326, 2011.
- [2] K. Keiji Kanazawa and J. G. Gordon II, "The oscillation frequency of a quartz resonator in contact with liquid," *Analytica Chimica Acta*, vol. 175, no. C, pp. 99–105, 1985.
- [3] T. Nomura and M. Okuhara, "Frequency shifts of piezoelectric quartz crystals immersed in organic liquids," *Analytica Chimica Acta*, vol. 142, pp. 281–284, 1982.
- [4] M. Yang, M. Thompson, and W. C. Duncan-Hewitt, "Interfacial properties and the response of the thickness-shear-mode acoustic wave sensor in liquids," *Langmuir*, vol. 9, no. 3, pp. 802–811, 1993.
- [5] A. Tsortos, G. Papadakis, and E. Gizeli, "Shear acoustic wave biosensor for detecting DNA intrinsic viscosity and conformation: a study with QCM-D," *Biosensors and Bioelectronics*, vol. 24, no. 4, pp. 836–841, 2008.
- [6] K. M. M. Aung, X. Ho, and X. Su, "DNA assembly on streptavidin modified surface: a study using quartz crystal microbalance with dissipation or resistance measurements," *Sensors and Actuators B: Chemical*, vol. 131, no. 2, pp. 371–378, 2008.
- [7] A. Doliška, V. Ribitsch, K. S. Kleinschek, and S. Strnad, "Viscoelastic properties of fibrinogen adsorbed onto poly(ethylene terephthalate) surfaces by QCM-D," *Carbohydrate Polymers*, vol. 93, no. 1, pp. 246–255, 2013.
- [8] F. Höök, B. Kasemo, T. Nylander, C. Fant, K. Sott, and H. Elwing, "Variations in coupled water, viscoelastic properties, and film thickness of a Mefp-1 protein film during adsorption and cross-linking: a quartz crystal microbalance with dissipation monitoring, ellipsometry, and surface plasmon resonance study," *Analytical Chemistry*, vol. 73, no. 24, pp. 5796–5804, 2001.
- [9] X.-L. Su and Y. Li, "A QCM immunosensor for *Salmonella* detection with simultaneous measurements of resonant frequency and motional resistance," *Biosensors and Bioelectronics*, vol. 21, no. 6, pp. 840–848, 2005.
- [10] K. A. Marx, T. Zhou, A. Montrone, D. McIntosh, and S. J. Braunhut, "Quartz crystal microbalance biosensor study of endothelial cells and their extracellular matrix following cell removal: evidence for transient cellular stress and viscoelastic changes during detachment and the elastic behavior of the pure matrix," *Analytical Biochemistry*, vol. 343, no. 1, pp. 23–34, 2005.
- [11] M. I. Ivanchenko, H. Kobayashi, E. A. Kulik, and N. B. Dobrova, "Studies on polymer solutions, gels and grafted layers using the quartz crystal microbalance technique," *Analytica Chimica Acta*, vol. 314, no. 1-2, pp. 23–31, 1995.
- [12] J. C. Munro and C. W. Frank, "Polyacrylamide adsorption from aqueous solutions on gold and silver surfaces monitored by the quartz crystal microbalance," *Macromolecules*, vol. 37, no. 3, pp. 925–938, 2004.
- [13] M. Yoshimoto, Y. Yuda, H. Aizawa, H. Sato, and S. Kurosawa, "Dynamic properties of the polyethylene glycol molecules on the oscillating solid-liquid interface," *Analytica Chimica Acta*, vol. 731, pp. 82–87, 2012.
- [14] S. M. Notley, M. Eriksson, and L. Wågberg, "Visco-elastic and adhesive properties of adsorbed polyelectrolyte multilayers determined in situ with QCM-D and AFM measurements," *Journal of Colloid and Interface Science*, vol. 292, no. 1, pp. 29–37, 2005.
- [15] C. E. Reed, K. K. Kanazawa, and J. H. Kaufman, "Physical description of a viscoelastically loaded AT-cut quartz resonator," *Journal of Applied Physics*, vol. 68, no. 5, pp. 1993–2001, 1990.
- [16] S. J. Martin, V. E. Granstaff, and G. C. Frye, "Characterization of a quartz crystal microbalance with simultaneous mass and liquid loading," *Analytical Chemistry*, vol. 63, no. 20, pp. 2272–2281, 1991.
- [17] H. L. Bandey, "Modeling the responses of thickness-shear mode resonators under various loading conditions," *Analytical Chemistry*, vol. 71, no. 11, pp. 2205–2214, 1999.
- [18] M. Rodahl, F. Höök, and B. Kasemo, "QCM operation in liquids: An explanation of measured variations in frequency and Q factor with liquid conductivity," *Analytical Chemistry*, vol. 68, no. 13, pp. 2219–2227, 1996.
- [19] R. Lucklum, G. Behling, R. W. Cernosek, and S. J. Martin, "Determination of complex shear modulus with thickness shear mode resonators," *Journal of Physics D: Applied Physics*, vol. 30, no. 3, pp. 346–356, 1997.
- [20] D. Johannsmann, K. Mathauer, G. Wegner, and W. Knoll, "Viscoelastic properties of thin films probed with a quartz-crystal resonator," *Physical Review B*, vol. 46, no. 12, pp. 7808–7815, 1992.
- [21] D. Johannsmann, J. Grüner, J. Wesser, K. Mathauer, G. Wegner, and W. Knoll, "Visco-elastic properties of thin films probed with a quartz crystal resonator," *Thin Solid Films*, vol. 210-211, part 2, pp. 662–665, 1992.
- [22] M. Andersson, J. Andersson, A. Sellborn, M. Berglin, B. Nilsson, and H. Elwing, "Quartz crystal microbalance-with dissipation monitoring (QCM-D) for real time measurements of blood

- coagulation density and immune complement activation on artificial surfaces,” *Biosensors & Bioelectronics*, vol. 21, no. 1, pp. 79–86, 2005.
- [23] Z. Parlak, C. Biet, and S. Zauscher, “Decoupling mass adsorption from fluid viscosity and density in quartz crystal microbalance measurements using normalized conductance modeling,” *Measurement Science and Technology*, vol. 24, no. 8, Article ID 085301, 2013.
- [24] S. Qin, X. Tang, L. Zhu, Y. Wei, X. Du, and D.-M. Zhu, “Viscoelastic signature of physisorbed macromolecules at the solid-liquid interface,” *Journal of Colloid and Interface Science*, vol. 383, no. 1, pp. 208–214, 2012.
- [25] A. Domack, O. Prucker, J. R uhe, and D. Johannsmann, “Swelling of a polymer brush probed with a quartz crystal resonator,” *Physical Review E—Statistical Physics, Plasmas, Fluids, and Related Interdisciplinary Topics*, vol. 56, no. 1, pp. 680–689, 1997.
- [26] B. Wu, K. Wu, P. Wang, and D.-M. Zhu, “Adsorption kinetics and adsorption isotherm of poly(N-isopropylacrylamide) on gold surfaces studied using QCM-D,” *Journal of Physical Chemistry C*, vol. 111, no. 3, pp. 1131–1135, 2007.
- [27] D.-M. Zhu, J. Fang, B. Wu, and X. Du, “Viscoelastic response and profile of adsorbed molecules probed by quartz crystal microbalance,” *Physical Review E: Statistical, Nonlinear, and Soft Matter Physics*, vol. 77, no. 3, Article ID 031605, 2008.
- [28] P. Wang, J. Fang, S. Qin, Y. Kang, and D. M. Zhu, “Molecular weight dependence of viscosity and shear modulus of polyethylene glycol (PEG) solution boundary layers,” *Journal of Physical Chemistry C*, vol. 113, no. 31, pp. 13793–13800, 2009.
- [29] S. J. Geelhood, C. W. Frank, and K. Kanazawa, “Transient quartz crystal microbalance behaviors compared,” *Journal of the Electrochemical Society*, vol. 149, no. 1, pp. H33–H38, 2002.
- [30] H. Muramatsu, E. Tamiya, and I. Karube, “Computation of equivalent circuit parameters of quartz crystals in contact with liquids and study of liquid properties,” *Analytical Chemistry*, vol. 60, no. 19, pp. 2142–2146, 1988.
- [31] A. Saluja and D. S. Kalonia, “Measurement of fluid viscosity at microliter volumes using quartz impedance analysis,” *AAPS PharmSciTech*, vol. 5, no. 3, article e47, 2004.
- [32] A. L. Kipling and M. Thompson, “Network analysis method applied to liquid-phase acoustic wave sensors,” *Analytical Chemistry*, vol. 62, no. 14, pp. 1514–1519, 1990.
- [33] D. Wang, P. Mousavi, P. J. Hauser, W. Oxenham, and C. S. Grant, “Quartz crystal microbalance in elevated temperature viscous liquids: temperature effect compensation and lubricant degradation monitoring,” *Colloids and Surfaces A: Physicochemical and Engineering Aspects*, vol. 268, no. 1–3, pp. 30–39, 2005.
- [34] S. J. Martin, G. C. Frye, and K. O. Wessendorf, “Sensing liquid properties with thickness-shear mode resonators,” *Sensors and Actuators A: Physical*, vol. 44, no. 3, pp. 209–218, 1994.
- [35] A. Itoh and M. Ichihashi, “A frequency of the quartz crystal microbalance (QCM) that is not affected by the viscosity of a liquid,” *Measurement Science and Technology*, vol. 19, no. 7, Article ID 075205, 2008.
- [36] N.-J. Cho, J. N. D’Amour, J. Stalgren, W. Knoll, K. Kanazawa, and C. W. Frank, “Quartz resonator signatures under Newtonian liquid loading for initial instrument check,” *Journal of Colloid and Interface Science*, vol. 315, no. 1, pp. 248–254, 2007.
- [37] I. Teraoka, *Polymer Solutions*, John Wiley & Sons, New York, NY, USA, 2002.
- [38] P. A. Albertson, *Partition of Cell Particles and Macromolecules*, John Wiley & Sons, New York, NY, USA, 1986.
- [39] R. Webster, V. Elliott, B. K. Park, D. Walker, M. Hankin, and P. Taupin, “PEG and PEG conjugates toxicity: towards an understanding of the toxicity of PEG and its relevance to PEGylated biologicals,” in *PEGylated Protein Drugs: Basic Science and Clinical Application*, F. M. Veronese, Ed., pp. 127–146, Birkh user, Basel, Switzerland, 2009.
- [40] D. De Kee, J. Stastna, and M. B. Powley, “Investigation of a new complex viscosity model,” *Journal of Non-Newtonian Fluid Mechanics*, vol. 26, no. 2, pp. 149–160, 1987.
- [41] F. H ok, M. Rodahl, P. Brzezinski, and B. Kasemo, “Energy dissipation kinetics for protein and antibody-antigen adsorption under shear oscillation on a quartz crystal microbalance,” *Langmuir*, vol. 14, no. 4, pp. 729–734, 1998.
- [42] G. McHale, R. L ucklum, M. I. Newton, and J. A. Cowen, “Influence of viscoelasticity and interfacial slip on acoustic wave sensors,” *Journal of Applied Physics*, vol. 88, no. 12, pp. 7304–7312, 2000.
- [43] K. K. Kanazawa, “Steady state and transient QCM solutions at the metal—solution interface,” *Journal of Electroanalytical Chemistry*, vol. 524, pp. 103–109, 2002.



